Electronic Supplementary Information

Tuning the Local Coordination Environment of Fe–N–C Catalysts via Sulfur Doping for Enhanced Oxygen Reduction

Sanjit Kumar Parida,[†,] * Hrudananda Jena[‡]

[†] Surface & Sensors Studies Division, Materials Science Group, Indira Gandhi Centre for Atomic Research, A CI of Homi Bhabha National Institute, Kalpakkam 603102, Tamilnadu, India

[‡] Materials Chemistry Division, Materials Chemistry and Metal Fuel Cycle Group, Indira Gandhi Centre for Atomic Research, A CI of Homi Bhabha National Institute, Kalpakkam 603102, India

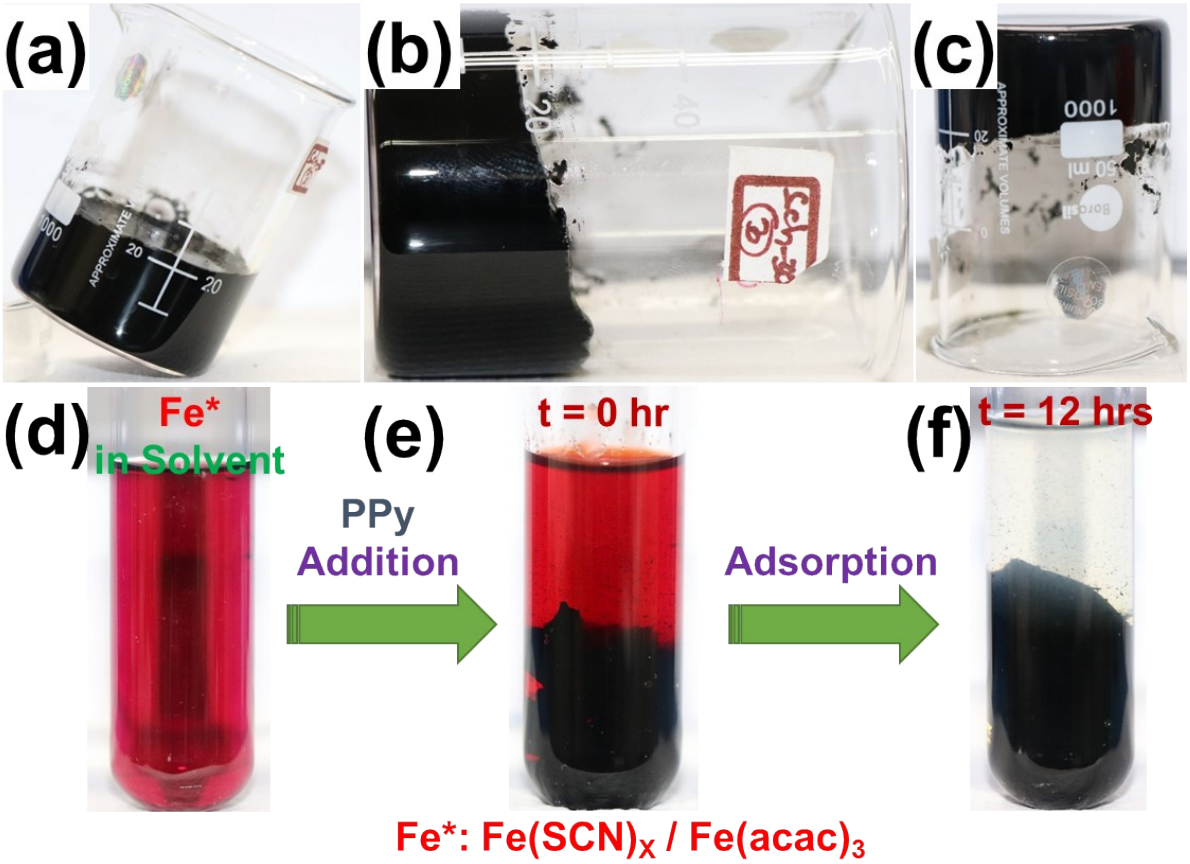

Fig. S1 (a, b, c) Photographs of PPy hydrogel and (d, e, f) $Fe(SCN)_x$ / $Fe(acac)_3$ loaded PPy at different time intervals.

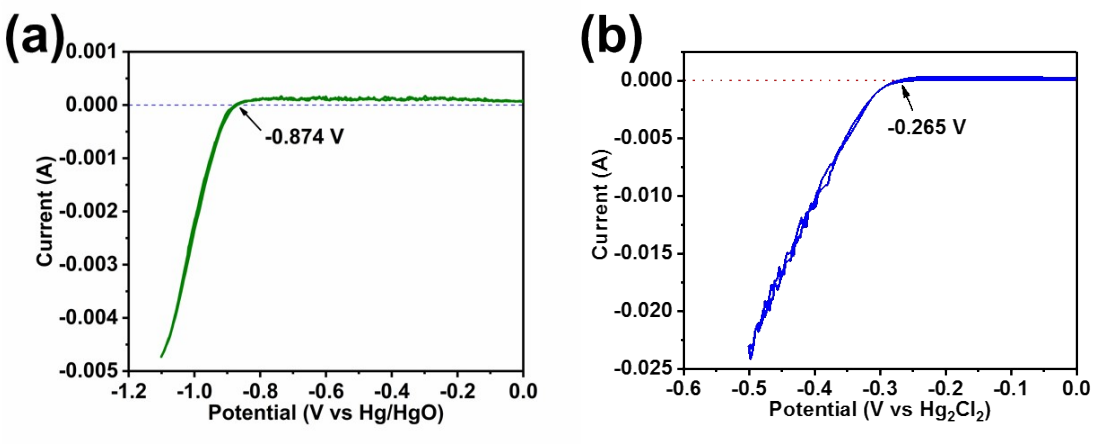

Fig. S2 Calibration graphs of (a) Hg/HgO and (b) SCE (Hg/Hg_2Cl_2) reference electrode.

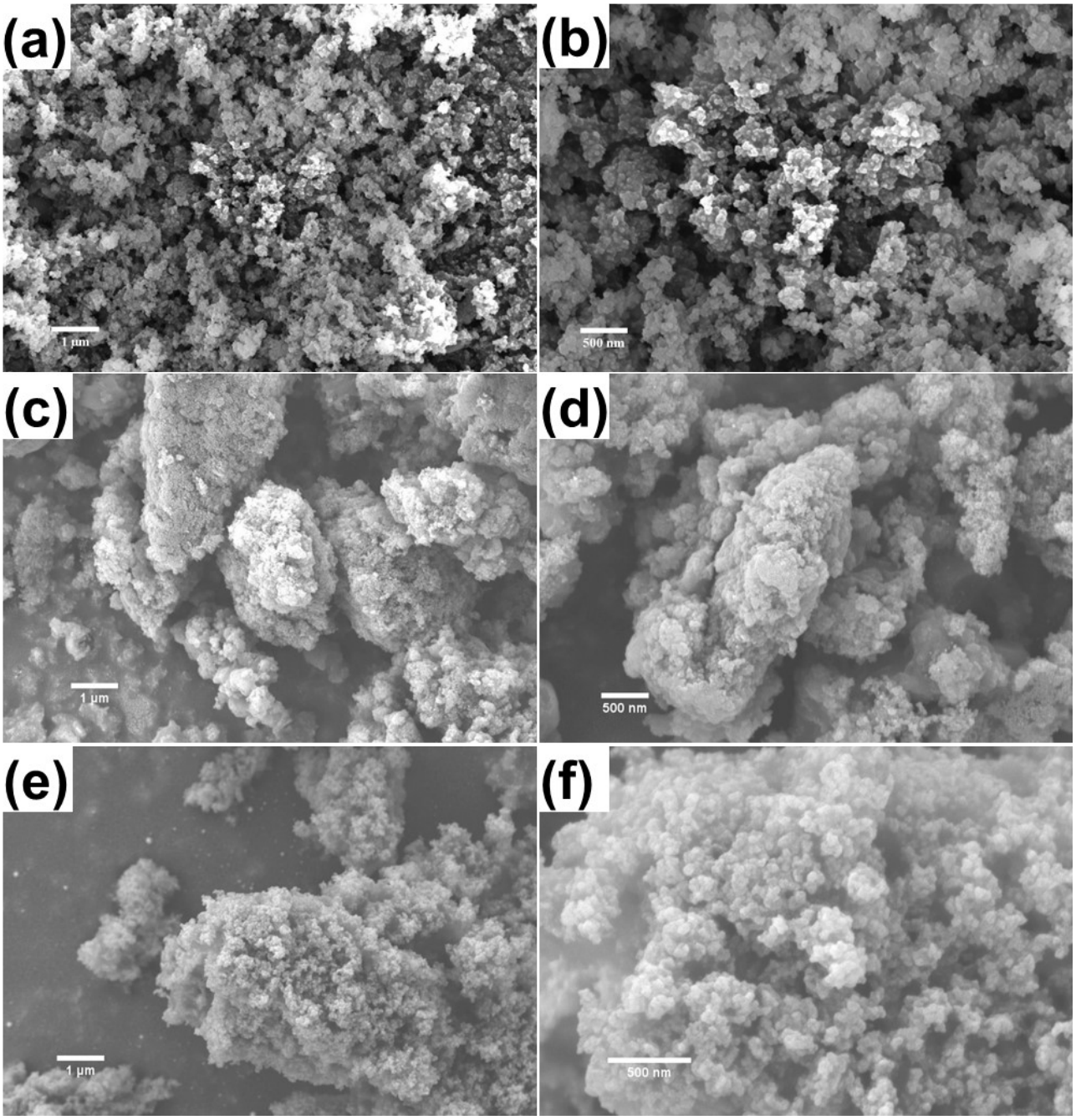

Fig. S3 FESEM images of (a)-(b) PPy, (c)-(d) $Fe(acac)_3$@PPy and (e)-(f) $Fe(SCN)_x$@PPy at different magnifications.

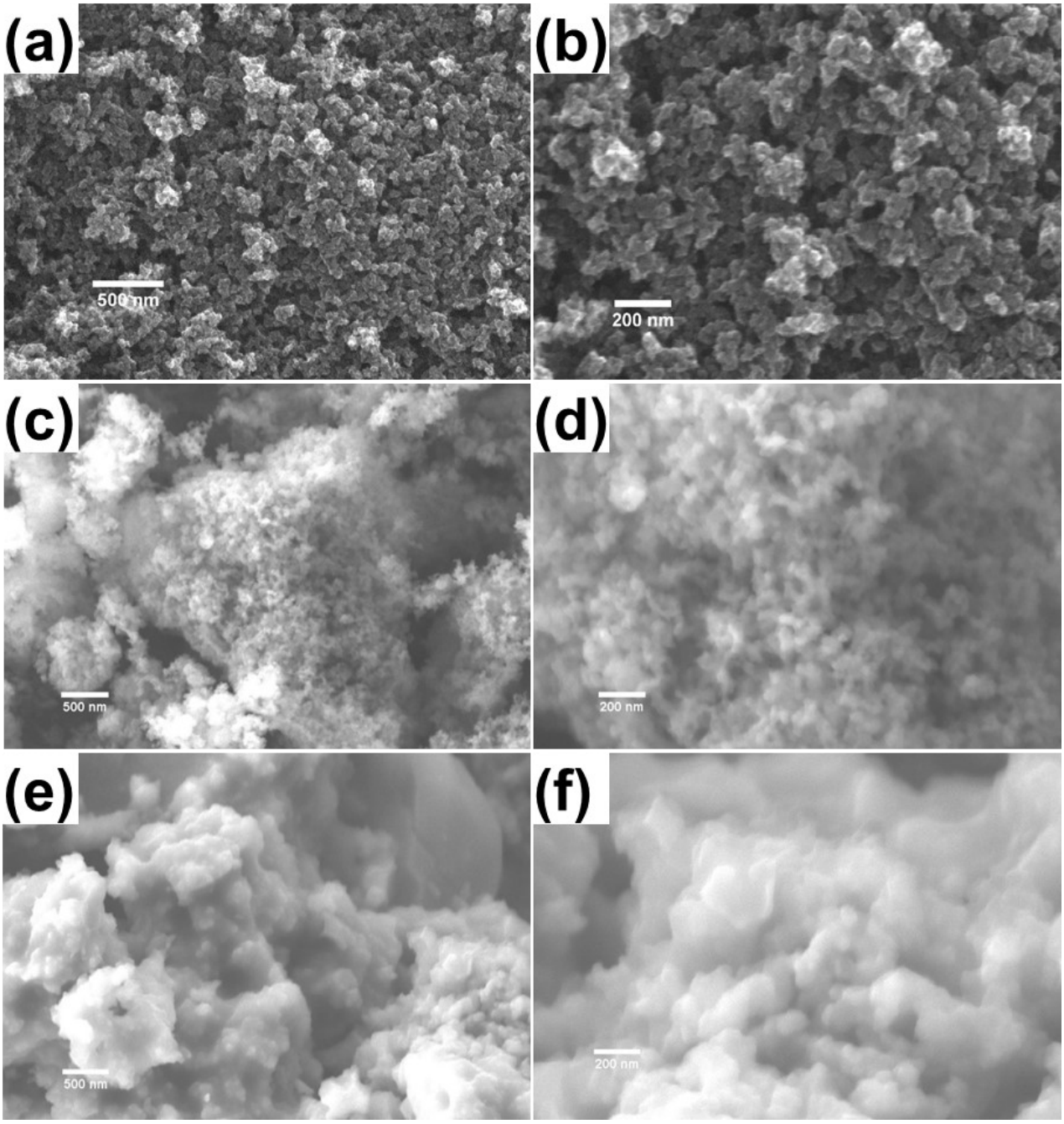

Fig. S4 FESEM images of (a)-(b) NC, (c)-(d) Fe-N-C and (e)-(f) Fe-N-C/S at different magnifications.

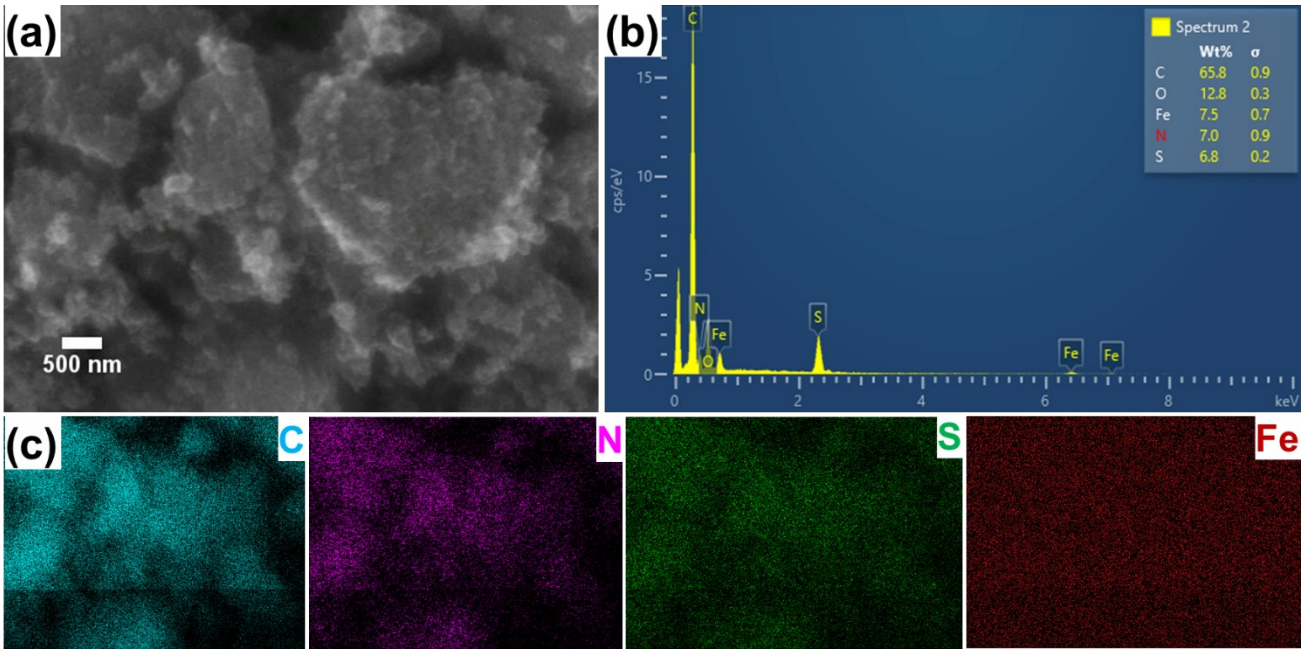

Fig. S5 (a) Representative FESEM image (b) EDX spectrum and (c) EDS elemental mapping results of Fe-N-C/S catalyst.

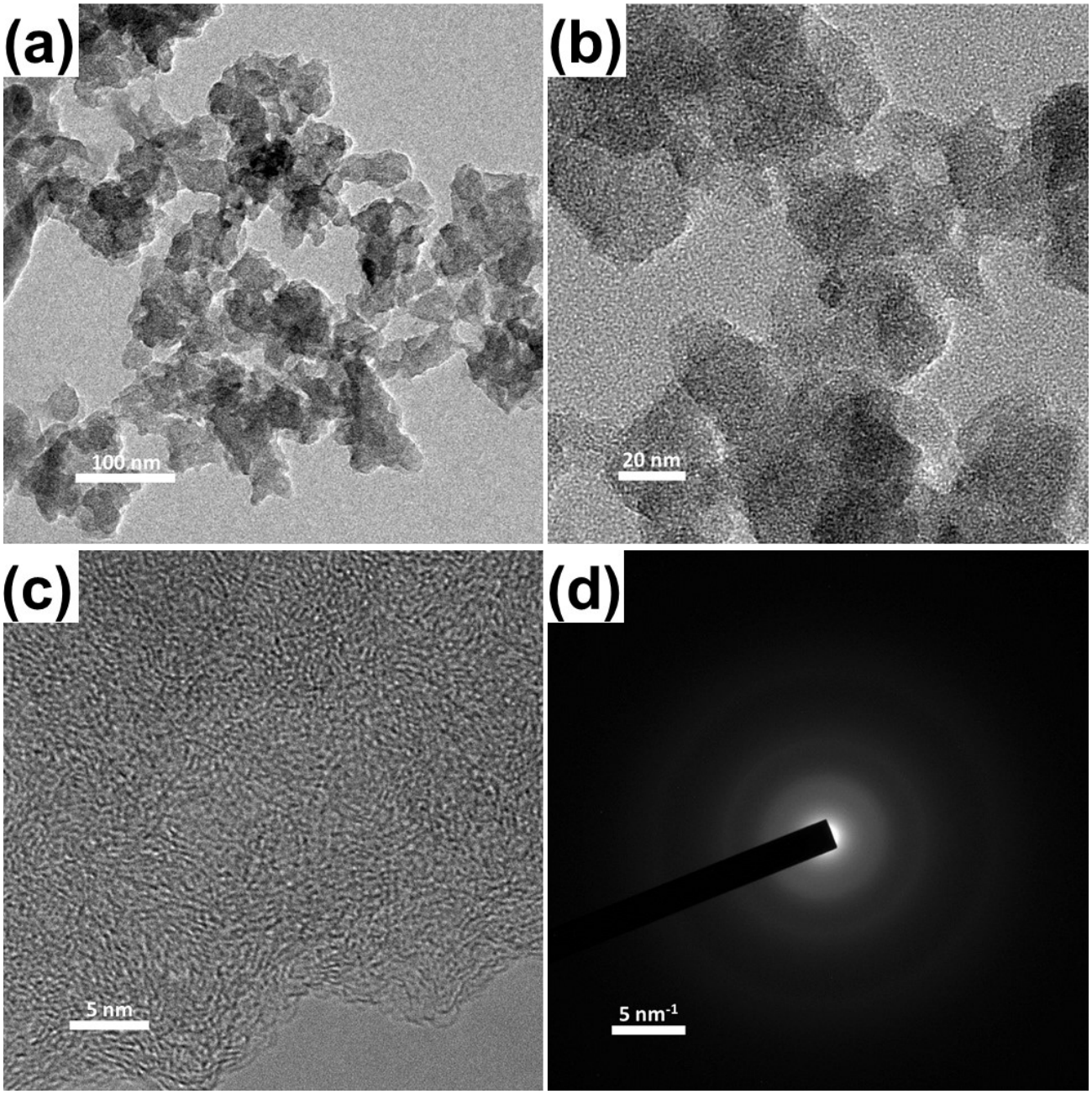

Fig. S6 (a)-(b) Representative STEM images (c) HRTEM image and (d) SAED pattern of Fe-N-C/S catalyst.

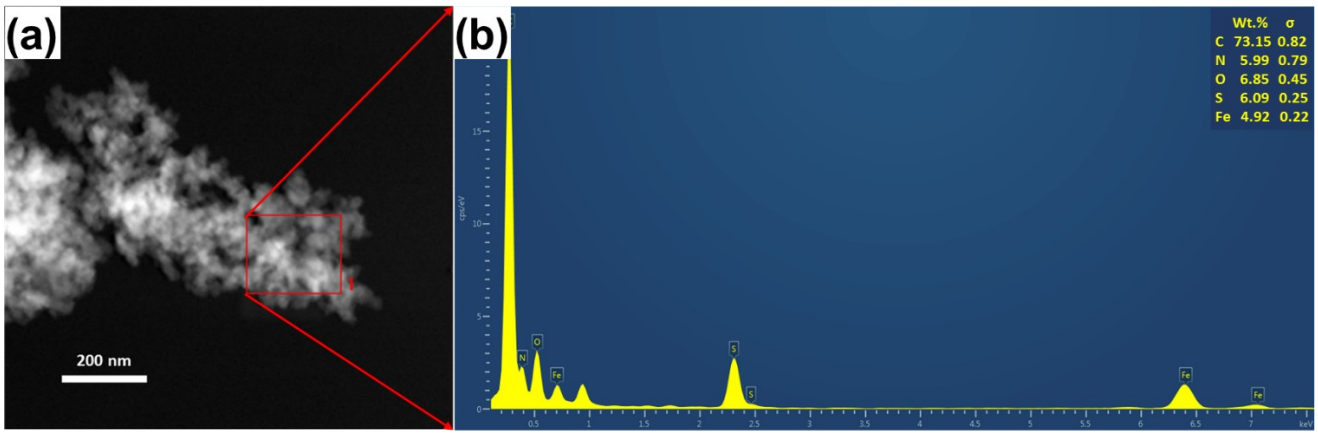

Fig. S7 (a) Representative STEM image with (b) EDX spectrum of Fe-N-C/S catalyst.

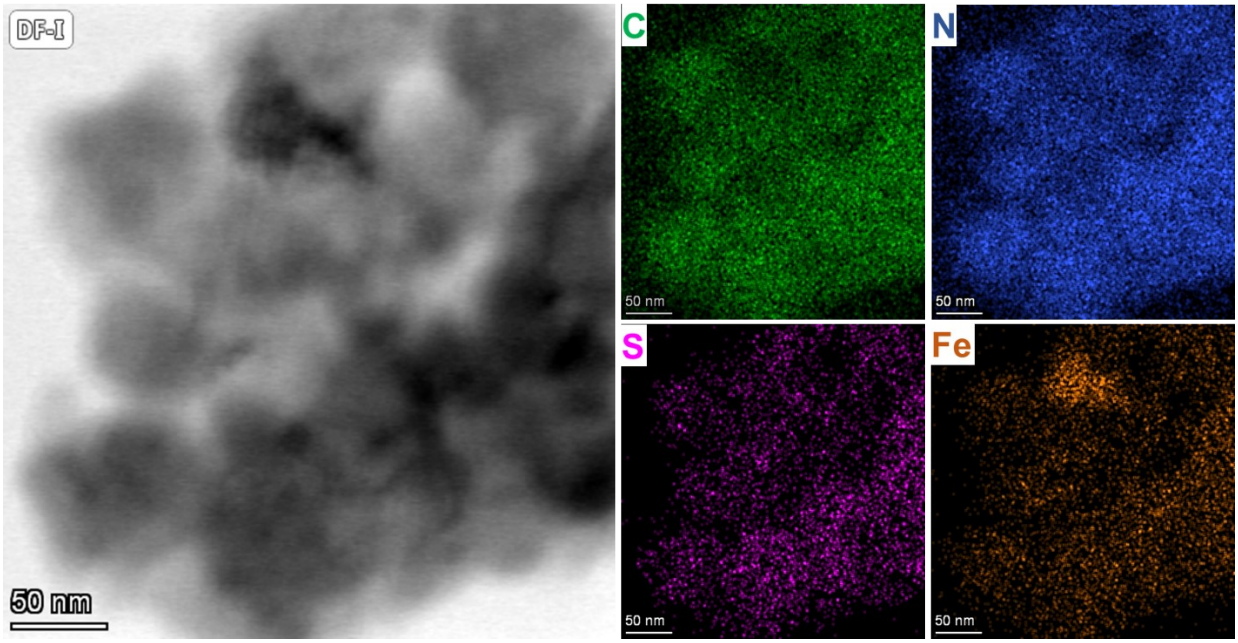

Fig. S8 Representative STEM image with corresponding EDS elemental mapping results of Fe-N-C/S catalyst.

Table S1. BET surface area and pore size of the catalysts.

Catalyst	SA_{BET} (m^2/g)	SA_{Micro} (m^2/g)	V_{Micro} (cc/g)	V_{Meso} (cc/g)	V_{Total} (cc/g)
NC	272.9	142.2	0.061	0.148	0.263
Fe-N-C	444.8	369.0	0.158	0.016	0.196
Fe-N-C/S	495.9	408.8	0.162	0.147	0.348

Table S2. Elemental composition of catalysts as obtained from XPS and ICP-OES.

Catalyst	XPS (at.%)			ICP-OCES (wt.%)
	N	S	Fe	Fe
NC	11.74	1.09	-	-
Fe-N-C	9.18	1.97	1.76	1.26
Fe-N-C/S	8.48	2.11	3.51	5.14

N.B. The S content of NC & Fe-N-C is attributable to SDS used during the synthesis of PPy.

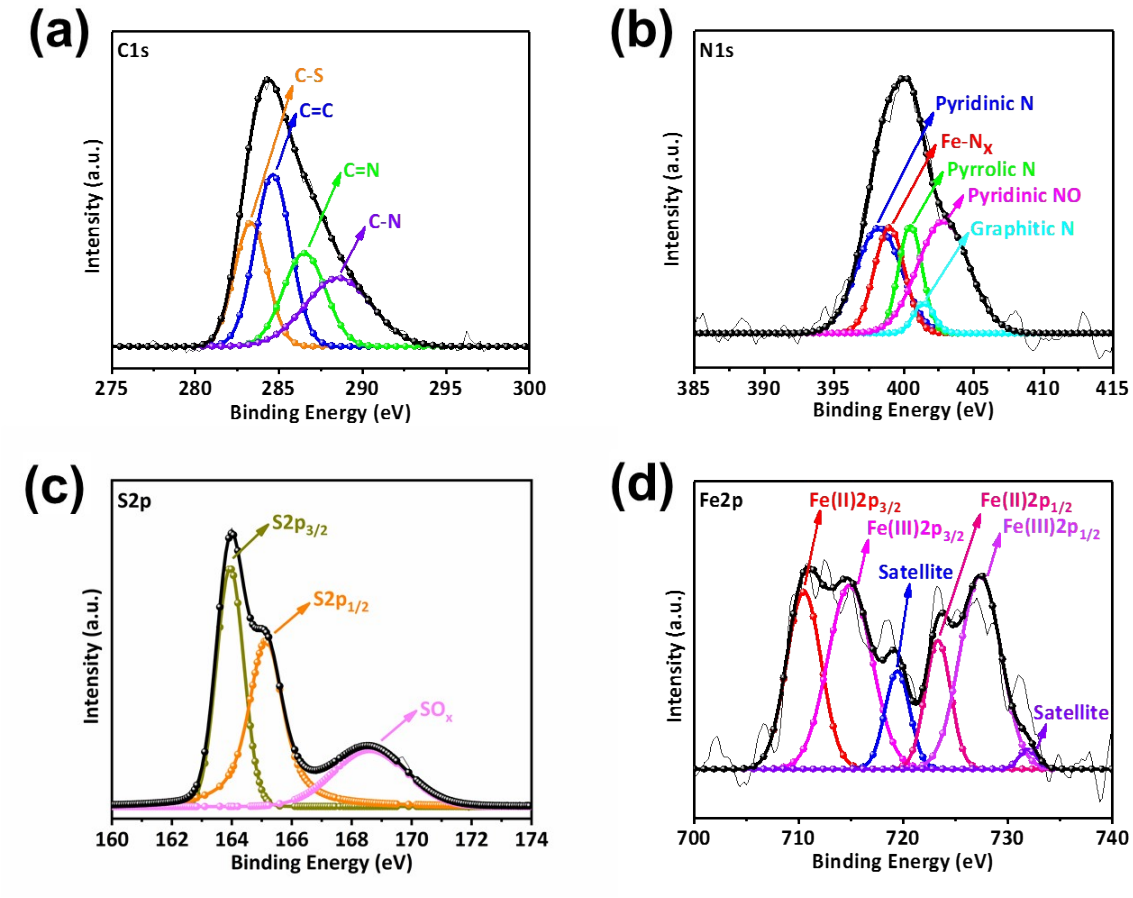

Fig. S9 High-resolution XPS spectra of (a) C1s, (b) N1s, (c) S2p and (d) Fe2p in Fe-N-C/S.

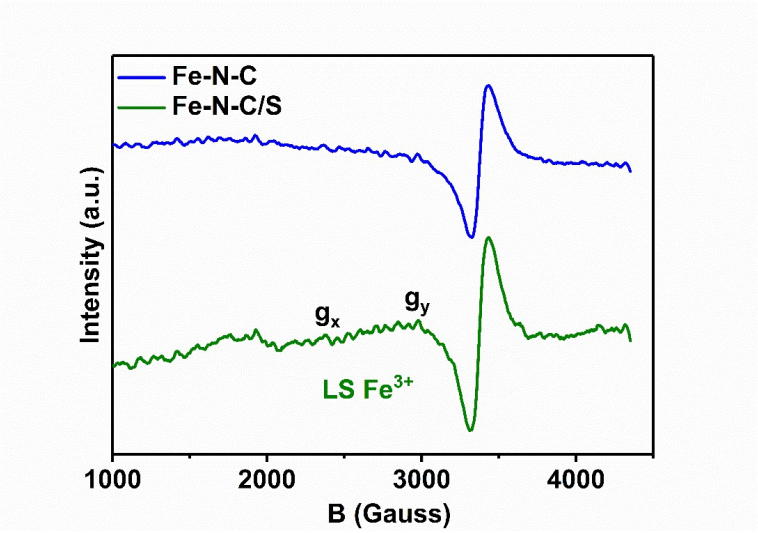

Fig. S10 EPR spectrum of the catalysts recorded at 100K.

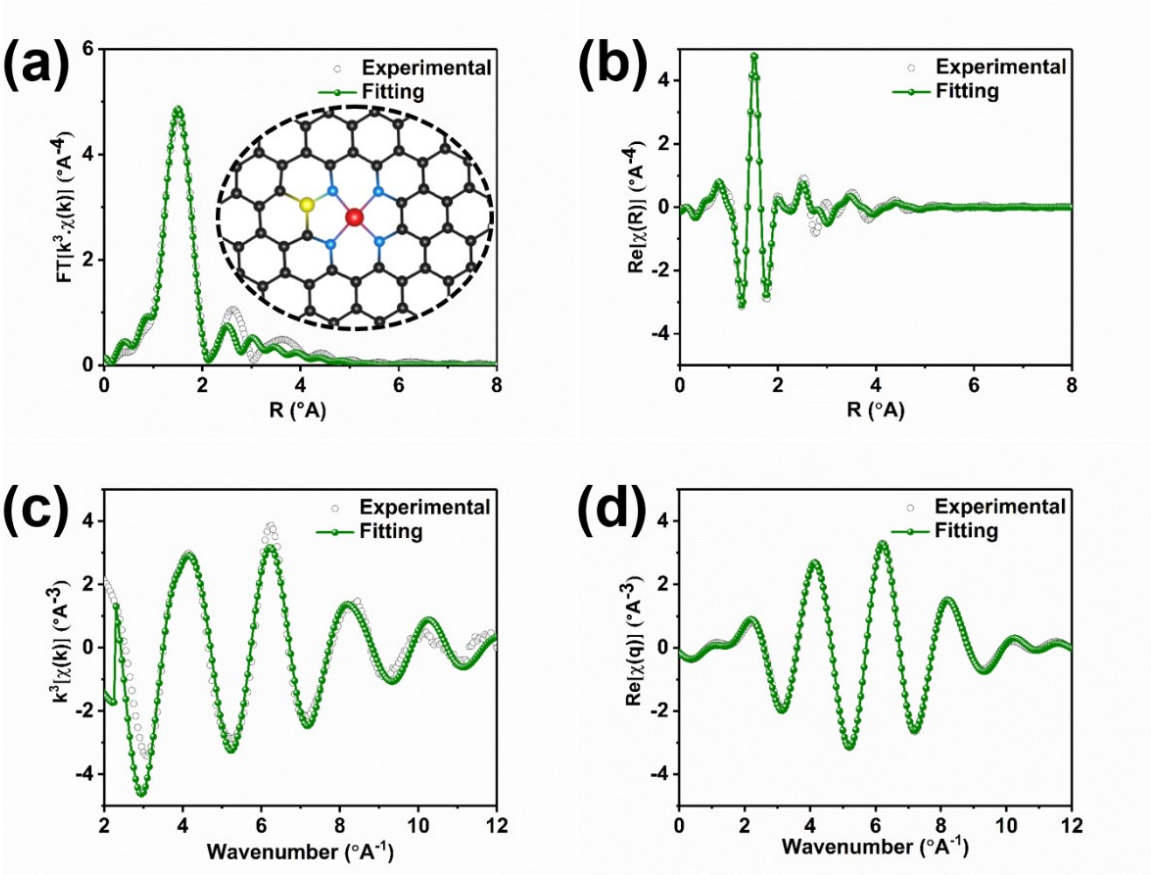

Fig. S11 The experimental and fitting curves of the EXAFS pattern of Fe-N-C/S with the model Fe-N_4-C_9S_1 structure in (a)-(b) R-space and (c)-(d) k-space.

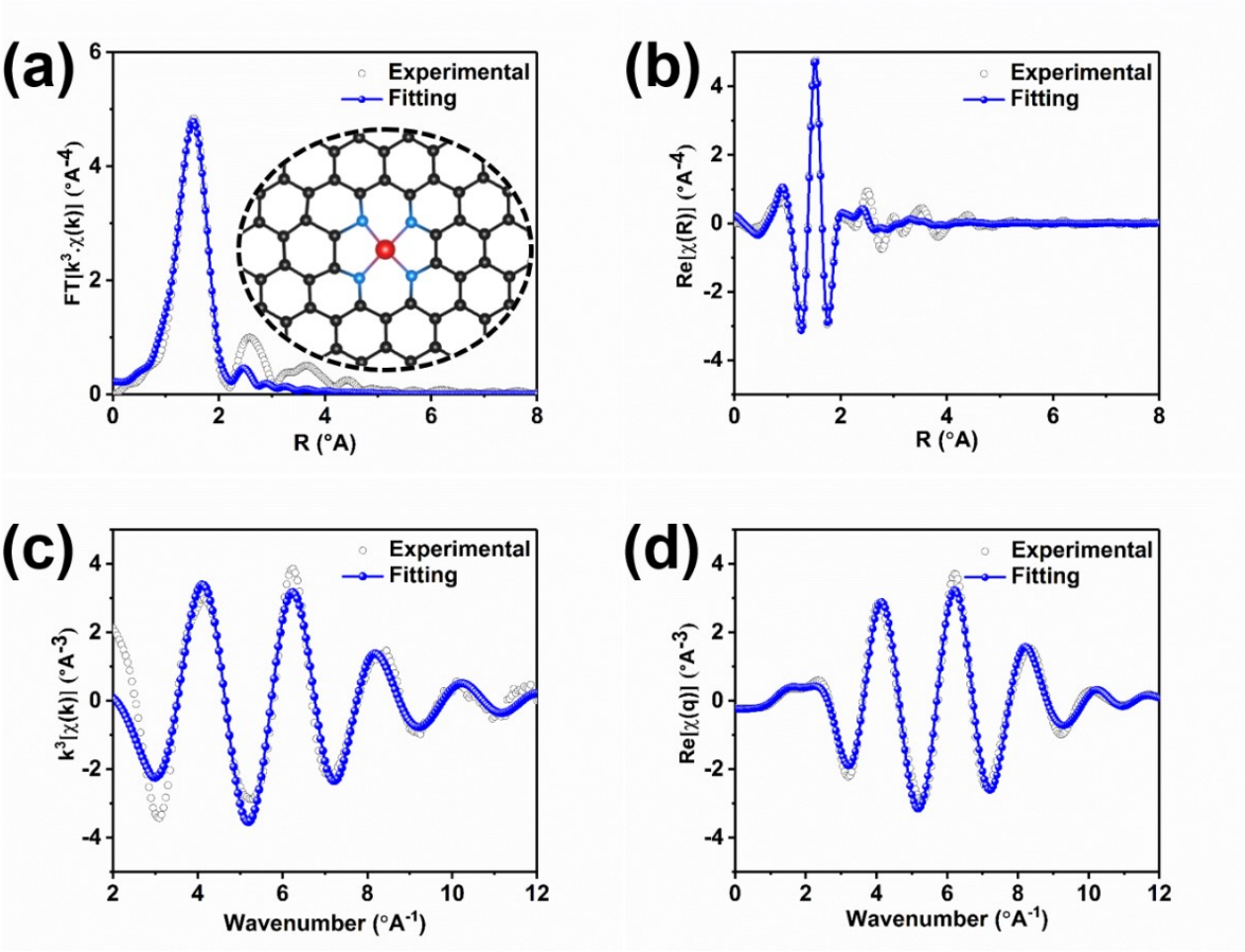

Fig. S12 The experimental and fitting curves of the EXAFS pattern of Fe-N-C/S with the model Fe-N_4-C_{10} structure in (a)-(b) R-space and (c)-(d) k-space.

Table S3. Fitting parameters of Fe K-edge EXAFS for Fe-N-C/S catalyst.

Sample	Model Structure	CN	R (°A)	σ^2 ($\times10^{-3}$)	ΔE_0 (eV)	R-factor
Fe-N-C/S	Fe-N_4-C_9S_1	4	1.89	9.1	4.4	0.0017
	Fe-N_4-C_{10}	4	1.99	12.6	-8.94	0.027

CN: coordination number; R: the distance between absorber and backscatter atoms (equals to the bond length of Fe-N); σ^2: the Debye-Waller factor value; ΔE_0: the inner potential correction to account for the difference in the inner potential between the sample and the reference compound.

Error bounds that characterize the structural parameters obtained by EXAFS spectroscopy were estimated as R ± 1%; σ^2 ± 20%; ΔE_0 ± 20%

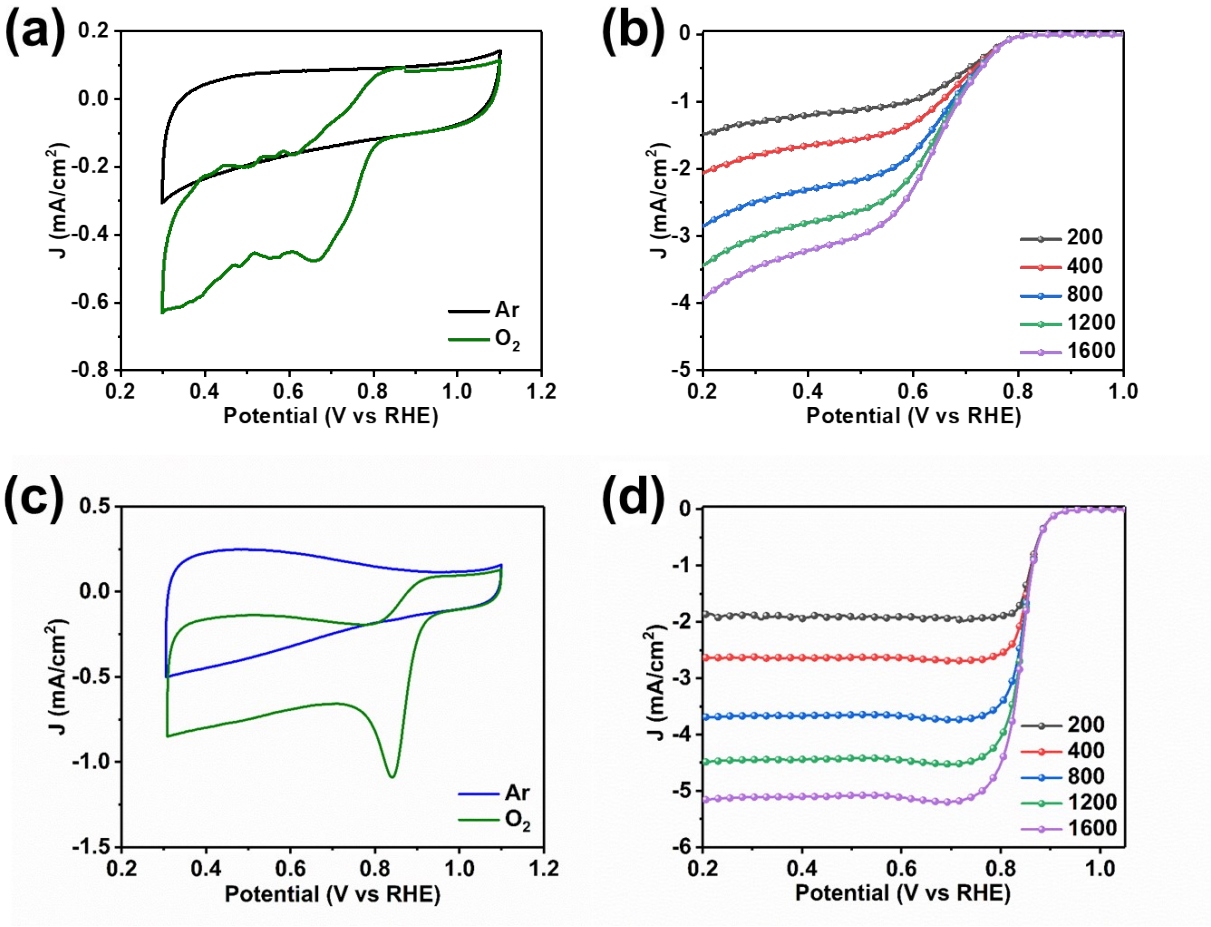

Fig. S13 Electrochemical performance of the catalysts showing (a) CV and (b) LSV curves of NC, (c) CV and (d) LSV curves of Fe-N-C in O_2 saturated 0.1M KOH.

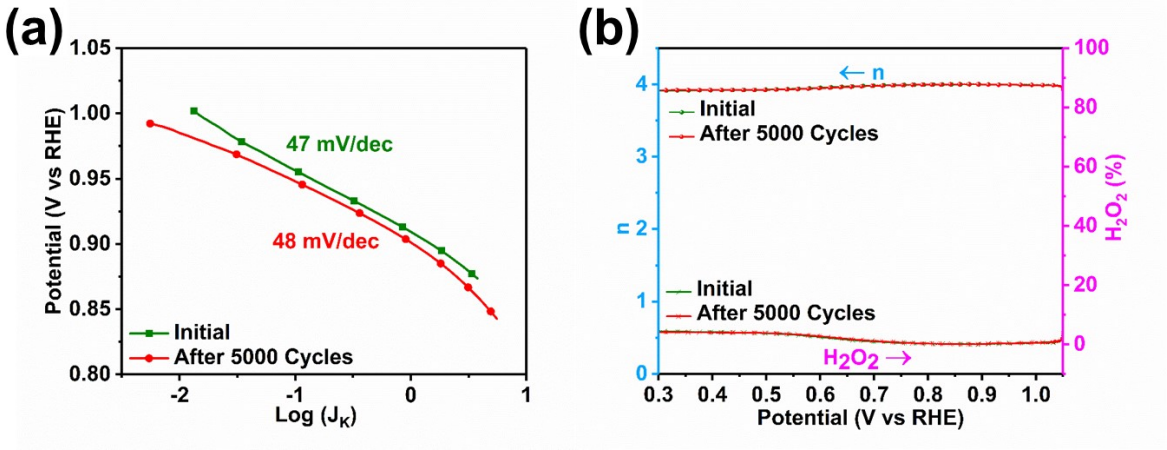

Fig. S14 (a) Tafel slopes and (b) RRDE results of Fe-N-C/S before and after potential cycling experiment for 5000 cycles in 0.1M KOH.

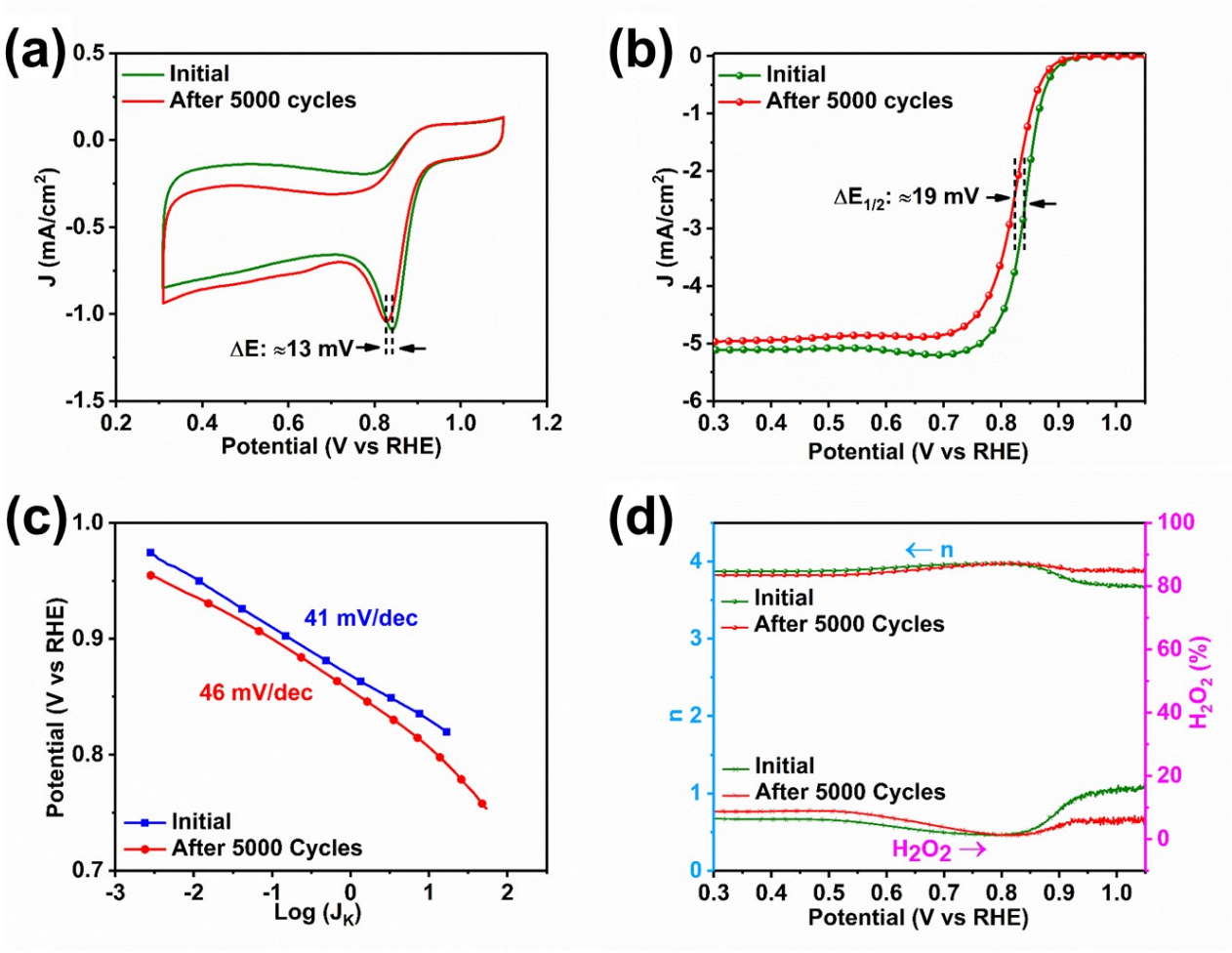

Fig. S15 (a) CV and (b) LSV curves (c) Tafel slopes and (d) RRDE results of Fe-N-C before and after potential cycling experiment for 5000 cycles in 0.1M KOH.

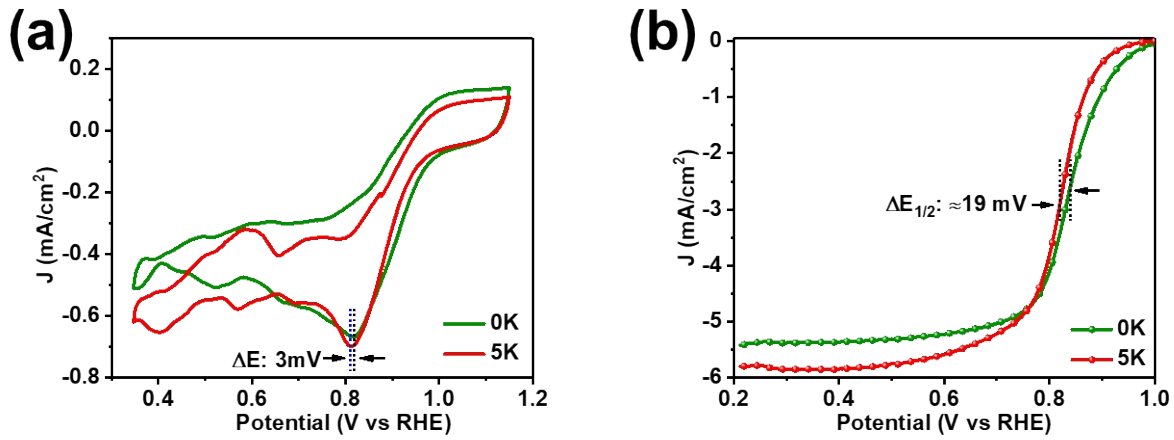

Fig. S16 (a) CV and (b) LSV curves of Pt/C after potential cycling experiment for 5000 cycles in 0.1M KOH.

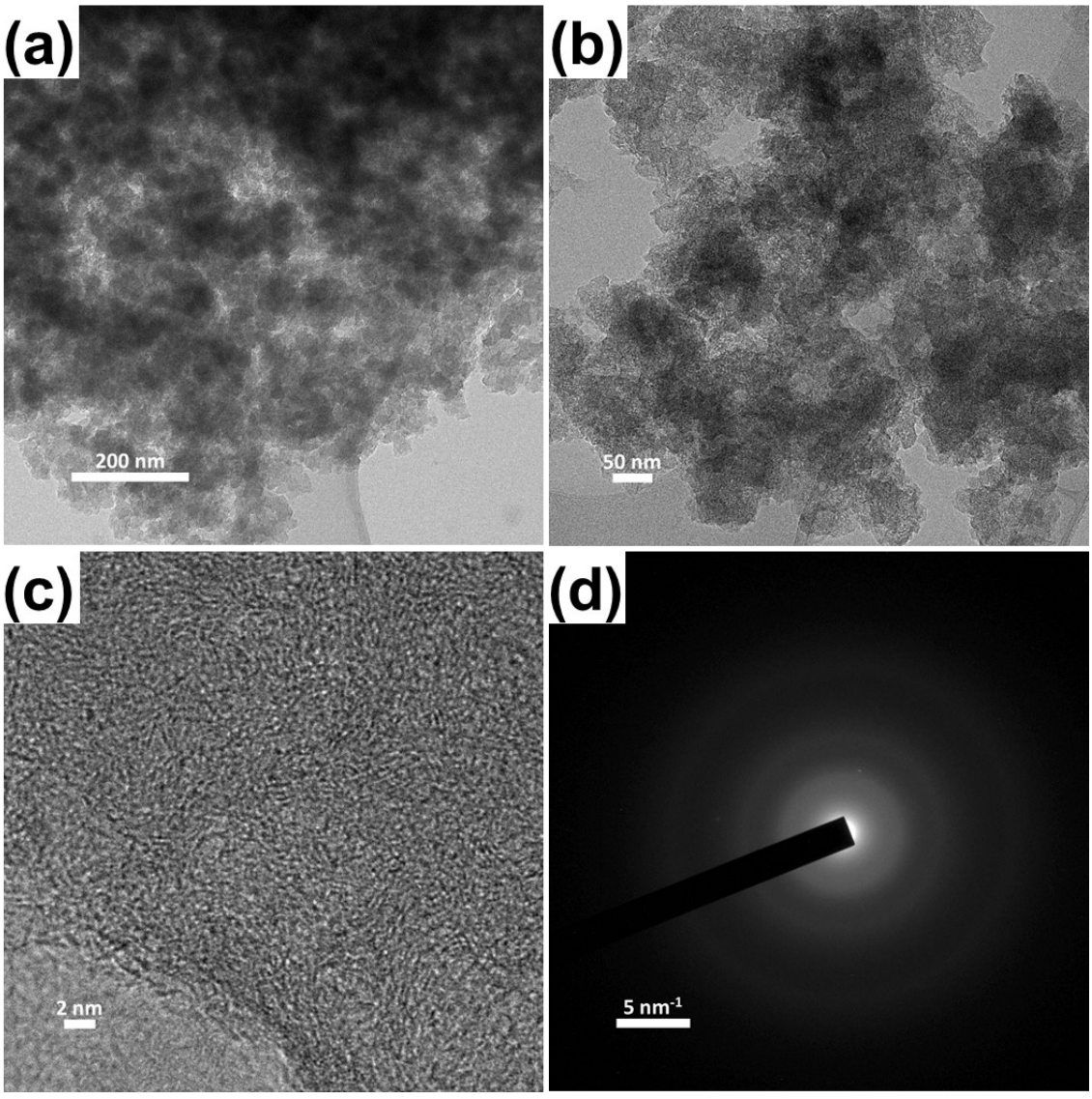

Fig. S17 (a)-(b) Representative STEM images (c) HRTEM image and (d) SAED pattern of Fe-N-C/S catalyst after potential cycling experiment.

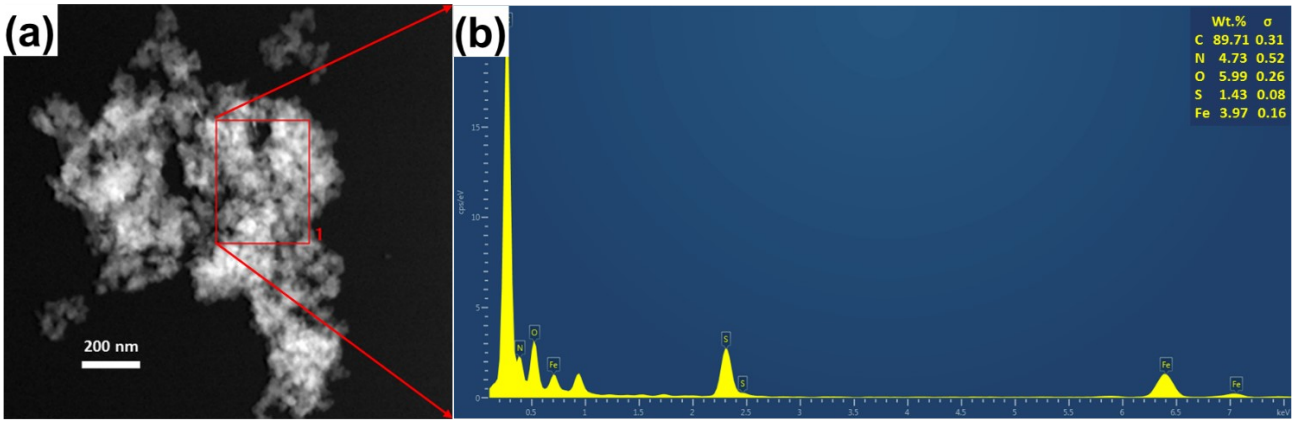

Fig. S18 (a) Typical STEM image with (b) EDX spectrum of Fe-N-C/S after potential cycling experiment.

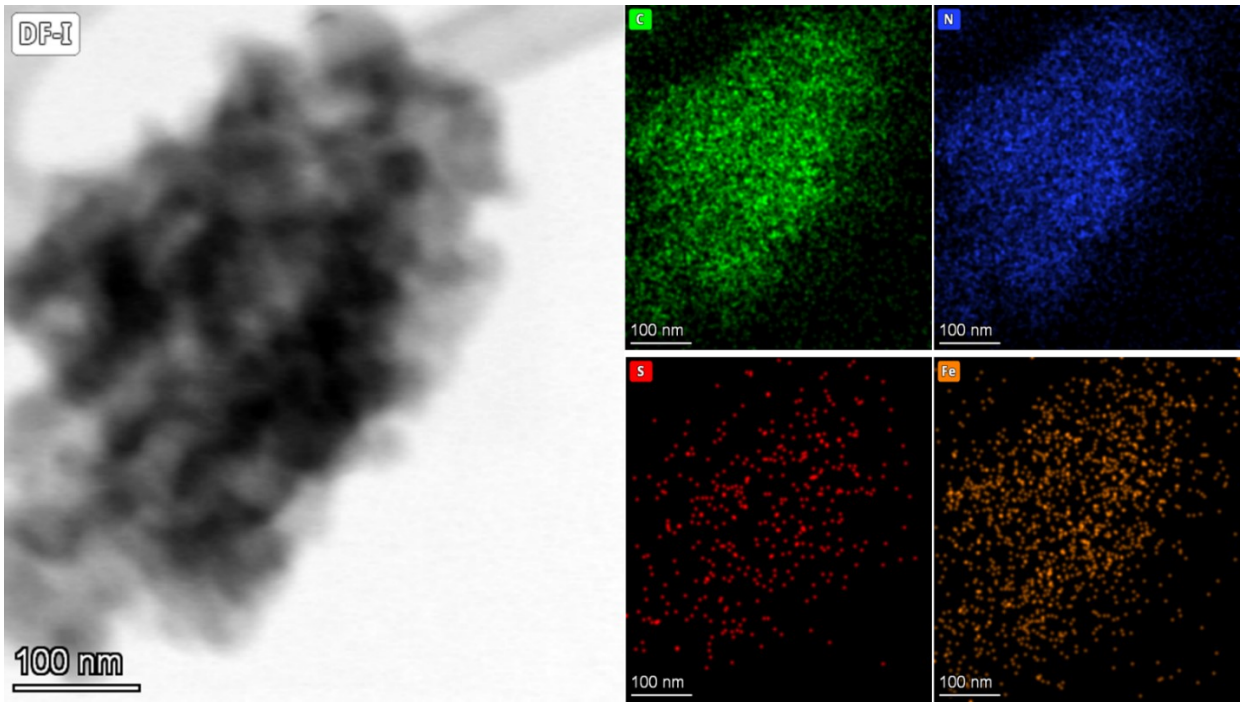

Fig. S19 Representative STEM image with corresponding EDS elemental mapping results of Fe-N-C/S catalyst after potential cycling experiment.

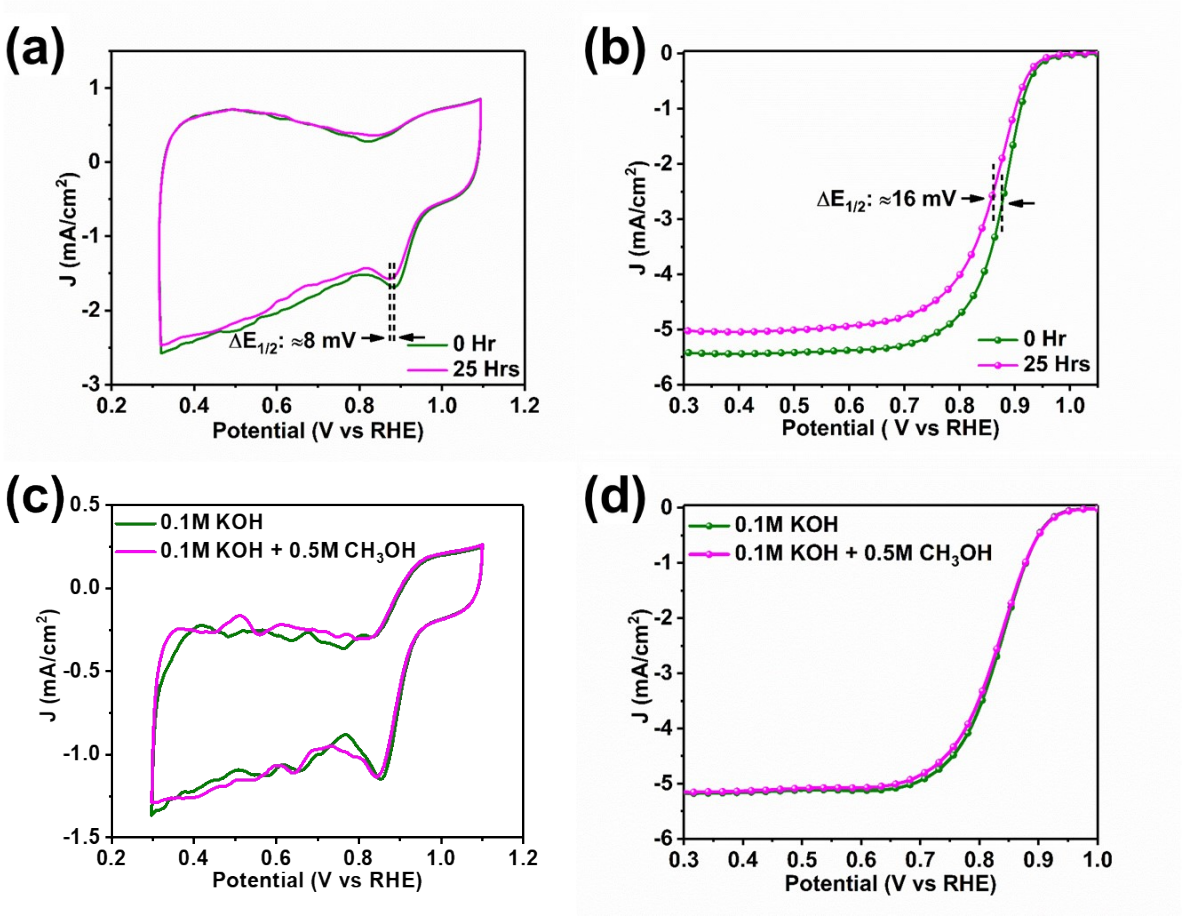

Fig. S20 (a) CV and (b) LSV curves of Fe-N-C/S after chronoamperometric response at 0.8V vs RHE for 25 Hrs. (c) CV and (d) LSV curves of Fe-N-C/S during methanol tolerance test.

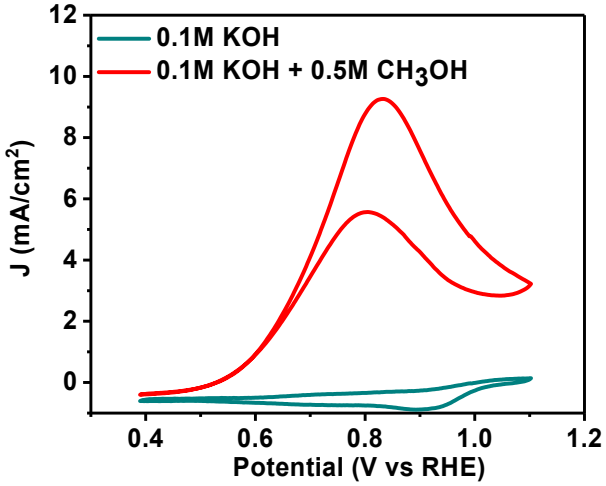

Fig. S21 Methanol tolerance test result of Pt/C showing CV in O_2 saturated 0.1M KOH and 0.1M KOH+0.5M CH_3OH.

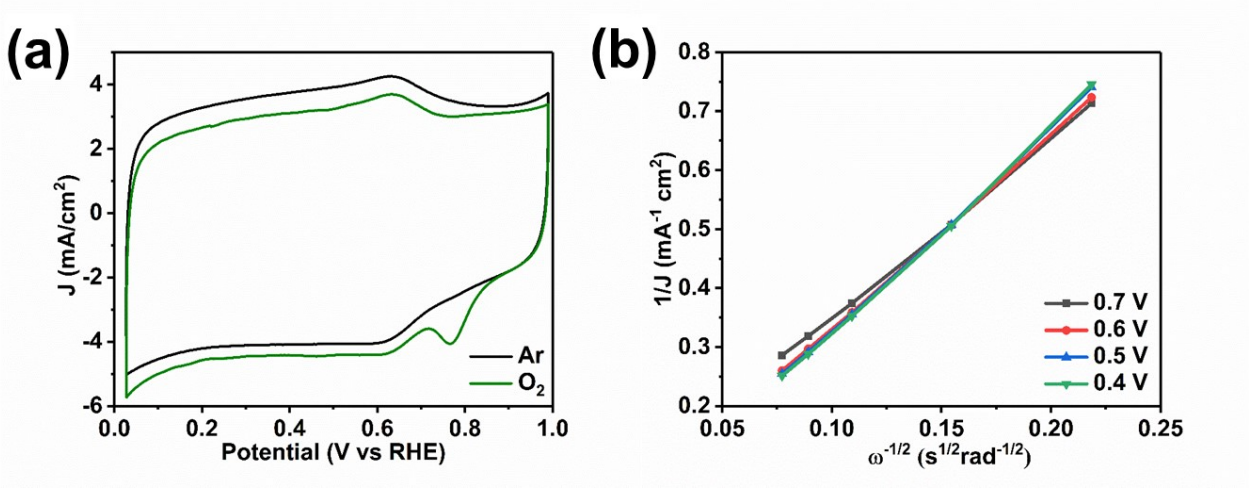

Fig. S22 Electrochemical performance of the catalyst showing (a) CV and (d) K-L plot of Fe-N-C/S in 0.5M H_2SO_4.

Table S4. Review of ORR activity of electronically engineered Fe SACs in 0.1M KOH as reported in recent literature.

Catalyst	Fe Content	Loading (μg/cm²)	E_{on} (V vs RHE)	$E_{1/2}$ (V vs RHE)	J_K (mA/cm²)	Ref.
Fe-N-C/S	**5.14 wt%**	**400**	**1.017**	**0.860**	**47.7 @ 0.7 V**	**This work**
P/Fe-N-C	1.7 wt%	600	1.010	0.900	25.4 @ 0.85 V	[1] J. Am. Chem. Soc. 2023, 145, 6, 3647–3655
Fe_1-$N_4S_{1.3}C$	0.83 at%	203	0.930	0.810	5.45	[2] Angew.Chem. Int. Ed. 2021, 60,25404–25410
Fe,Mn/N–C	2.3 wt%	100	0.979	0.928	7.04	[3] Nat Commun 12, 1734 (2021)
Fe-N/P-C-700	1.03 at%	600	0.941	0.867	24.49	[4] J . Am . Chem . Soc . 2020, 142, 2404-2412.
Fe_{SA}/B,N-CNT	0.1 at%	-	1.070	0.933	62.57 @ 0.85 V	[5] J. Mater. Chem. A, 2019,7, 20952 –20957
SA-Fe-HPC	0.80 at%	100	-	0.890	3.72 @ 0.90 V	[6] Angew. Chem. Int. Ed., 2018, 57, 9038-9043
$FeCl_1N_4$/CNS	1.5 wt%	501	-	0.921	41.11 @ 0.85 V	[7] Energy Environ. Sci. 2018, 11, 2348
meso/micro-FeCo-N_x-CN-30	0.40 at%	1000	0.954	0.886	-	[8] Angew. Chem. Int. Ed. 2018, 57, 1856 –1862
S,N-Fe/N/C-CNT	0.8 at%	600	-	0.850	-	[9] Angew. Chem. Int. Ed. 2016, 55,1–6
Fe/Co-NpGr	0.29 at%	707	0.930	-	-	[10] Adv. Funct. Mater. 2016, 26, 2150–2162
Fe–P-900	1.9 at%	39.5	0.950	-	-	[11] J. Am. Chem. Soc. 2015, 137, 9, 3165–3168